sustainability

MDPI

Article

Zagros Grass Index—A New Vegetation Index to Enhance Fire Fuel Mapping: A Case Study in the Zagros Mountains

Iraj Rahimi [1,2,3], Lia Duarte [1,3,*] and Ana Cláudia Teodoro [1,3]

[1] Department of Geosciences, Environment and Spatial Planning, Faculty of Sciences, University of Porto, 4169-007 Porto, Portugal; iraj.amin@spu.edu.iq (I.R.); amteodor@fc.up.pt (A.C.T.)
[2] Darbandikhan Technical Institute, Sulaimani Polytechnic University, Wrme Street 327/76, Qrga, Sulaymaniyah 70-236, Iraq
[3] Institute of Earth Sciences, Faculty of Sciences, University of Porto, 4169-007 Porto, Portugal
* Correspondence: liaduarte@fc.up.pt

Abstract: Annually, the oak forests of the Zagros Mountains chains in western Iran and northeastern Iraq face recurring challenges posed by forest fires, particularly in the Kurdo–Zagrosian forests in western Iran and northeastern Iraq. Assessing fire susceptibility relies significantly on vegetation conditions. Integrating in situ data, Remote Sensing (RS) data, and Geographical Information Systems (GIS) integration presents a cost-effective and precise approach to capturing environmental conditions before, during, and after fire events, minimizing the need for extensive fieldwork. This study refines and applies the Zagros Grass Index (ZGI), a local vegetation index tailored to discern between grass-covered surfaces and tree canopies in Zagros forests, identifying the grass masses as the most flammable fuel type. Utilizing the Moderate Resolution Imaging Spectroradiometer (MODIS) Normalized Difference Vegetation Index (NDVI) product as input from 2013 to 2022, the ZGI aims to mitigate the influence of tree canopies by isolating NDVI values solely attributable to grass cover. By incorporating phenological characteristics of forest trees and grass species, the ZGI outperforms NDVI in mapping grass-covered areas crucial for the study region's fire susceptibility assessment. Results demonstrate a substantial overlap between ZGI-based maps and recorded fire occurrences, validating the efficacy of the index in fire susceptibility estimation.

Keywords: remote sensing; vegetation index; NDVI Zagros grass index (ZGI); forest fire; Kurdo–Zagrosian

check for updates

Citation: Rahimi, I.; Duarte, L.; Teodoro, A.C. Zagros Grass Index—A New Vegetation Index to Enhance Fire Fuel Mapping: A Case Study in the Zagros Mountains. *Sustainability* **2024**, *16*, 3900. https://doi.org/10.3390/su16103900

Academic Editor: Basu Bidroha

Received: 5 March 2024
Revised: 11 April 2024
Accepted: 24 April 2024
Published: 7 May 2024

Copyright: © 2024 by the authors. Licensee MDPI, Basel, Switzerland. This article is an open access article distributed under the terms and conditions of the Creative Commons Attribution (CC BY) license (https://creativecommons.org/licenses/by/4.0/).

1. Introduction

Forest fires pose significant environmental, economic, and human safety concerns in most forested regions globally [1–4]. Ecologically, fire is a pivotal factor influencing vegetation diversity and dynamics over time and space [1–5]. Civil protection agencies, governments, local authorities, and forestry corps are compelled to effectively manage forest fires and establish preparedness strategies to preserve biome services and ensure citizen safety [6–9]. While forest fires can arise naturally due to dry weather, volcanic eruptions, or lightning, human activities are the predominant factors, particularly during heightened water stress [10,11].

The forest areas and rangelands along the western and northern expanses of the Zagros Mountains (Iraq) chain have faced many fires since 2005. The forests in Marivan and Paveh, situated in the Kurdistan and Kermanshah provinces of western Iran, respectively, are particularly affected [12,13]. Furthermore, the provinces of Sulaymaniyah and Halabja in the Kurdistan Region (KR) of northern Iraq have witnessed a notable surge in fire incidents in recent years, especially since 2008 [10]. According to official reports and studies conducted, human activities are the most frequent ignition sources in these forested areas [13,14]. It is also reported that more than 90% of fires in the European Union (EU) are human-caused [15,16]. Given the valuable opportunity presented by satellite-based indices for

monitoring diverse Earth phenomena, Remote Sensing (RS) data and Geographic Information System (GIS) technology have become crucial tools for natural resource managers and researchers across government agencies, conservation organizations, and industry [17–19]. The integration of RS data/techniques and GIS facilitates the efficient and accurate analysis of wildfire dynamics, enabling informed decision-making processes for fire management and mitigation strategies [17,18]. The occurrence of fires, including their severity and duration, is intricately correlated to vegetation conditions [10,17,18], including critical dynamic factors such as Fuel Moisture Content (FMC) and Fuel Temperature (FT) [20,21]. Several studies have been conducted worldwide to classify and map land cover due to its vast and vital role in natural resource management [22], agriculture management [23], and biodiversity conservation [24], among others. Various researchers have tried differentiating and mapping vegetation species such as trees, shrubs, and grass species using RS data and techniques. Some studies have used Light Detection and Ranging (LiDAR) data with tree height information to differentiate these species since these vegetation types have different heights [23]. However, LiDAR data are not available everywhere and is expensive [25]. On the other hand, numerous recent studies have also used Deep Learning (DL) algorithms for land cover classification [26]. Accordingly, advanced DL techniques with high-resolution satellite data perform better than traditional methods for classifying land cover and detecting objects. Although DL algorithms achieve high accuracy, they need more diverse training data to be efficient in different situations. However, most are applied to high-resolution satellite images [26]. In the work of Saah et al. [22], DeepLabV3+, a semantic segmentation-based DL method, was employed to categorize three types of vegetation land covers (trees, shrubs, and grass) utilizing solely Sentinel-2 RGB images.

In contrast, other methods rely on Vegetation Indices (VIs) generated from multispectral images [27]. VIs allow the extraction of valuable information from plants' spectral characteristics, including biochemical characteristics, environmental factors, and soil properties [27]. These indices are crucial in estimating vegetation biomass, canopy height, percentage vegetation cover changes, plant health, and Leaf Area Index (LAI). Additionally, they aid in distinguishing between soil and vegetation and mitigating atmospheric and topographical influences when feasible [28]. Meshesha et al. [29] found a strong correlation between forage biomass and spectral indices by employing the Sentinel-2 Normalized Difference Vegetation Index (NDVI) and Enhanced Vegetation Index (EVI), integrated with ground sampling in Harshin district, Ethiopia, to develop a forage forecasting model. Fakhri et al. [30] introduced a novel vegetation index-based workflow. Within it, the multi-objective particle swarm optimization (MOPSO) algorithm was applied to optimize a set of broadband VIs to reach both objectives of greenness estimation and vegetation/non-vegetation classification in a small area of Zagros sparse woodlands. A new index was also developed by Qian et al. [31] and applied in Beijing, China, merging spectral and texture features to differentiate trees from grass in urban areas at a detailed level using high-resolution GeoEye-1 imagery. Another study in northwest (NW) Russia utilized hyperspectral data and vegetation phenology to differentiate tree species [32]. It was concluded that classification using multispectral data effectively improves accuracy compared to a single hyperspectral image. In another study area in Zagros [33], a study was conducted to generate an accurate land cover map for the Shirvan County forests, a part of Zagros forests in Western Iran, using Sentinel-2-derived NDVI, Google Earth imagery, and field data for protective management. The study proved that the Support Vector Machine (SVM) algorithm had the highest accuracy for the classification of Sentinel-2 data, with an overall accuracy of 81.33%. In a greater area, for the entire Zagros Mountains, a new empirical model was introduced for mapping land cover for the whole Zagros Mountains using Sentinel-2-derived NDVI [34]. Despite being so challenging, this study has effectively mapped the land cover (agriculture, build-up area, wooded area, plantation, bare soil, water, and rangeland) for its wide study area. Salar et al. [35] also used NDVI as well as other factors (such as slope gradient, slope aspect, elevation, distance to roads, and distance to rivers, among others) to estimate the susceptibility of fire occurrence in

the Qaradagh area of Iraqi KR using a logistic regression model and evaluate it using Receiver Operating Characteristic (ROC) curve and Area Under the Curve (AUC). This paper concluded that the approach is useful for monitoring shrubland, grassland, and cropland fires in similar areas. Other methods, such as Evidential Belief Function (EBF) and Weight Of Evidence (WOE), map fire risk, more precisely the probability of ignition, in Marivan County, KR (Iran) [36]. The performance of the models was evaluated using the ROC curve, proving that WOE and EBF are effective tools for mapping forest fires. Multicriteria analysis, such as Analytical Hierarchy Process (AHP) analysis, was also used in the Zarivar Lake region of Marivan district. Rasooli et al. [37] determined the main factors that influence fire occurrence, identified areas with a higher vulnerability to fire, and assessed that vulnerability using remote sensing data combined with GIS. In Iraq, however, some studies were also conducted for mapping land cover in KR using VIs and DL approaches [38,39]. Although several studies have employed satellite images for mapping land cover, a minority deal with differentiating grass species from wood species. If they do, they focus on urban areas using high-resolution images [22–39]. However, the grass species has not been disregarded completely, and it is mostly classified as a member of the rangeland class with other members such as shrubs. The land cover, vegetation dynamics, topography, and distance from the population center and road, in addition to many other static and dynamic factors, are considered key factors in the fire susceptibility assessment [40–42]. Deriving reliable information on fuel types is a major factor since fires need fuel to happen and propagate [40,41]. In studying fuel types, grass species have not been looked at only as an ecological factor but as the most flammable fuel type [40,41]. Notably, the NDVI has been widely employed to estimate vegetation phenology as well as its quality and growth condition [43–45]. NDVI, serving as an index of vegetation growth and coverage, finds extensive use in describing spatio-temporal characteristics of land use and land cover (LULC), including percent vegetation coverage [44–47]. However, the NDVI cannot differentiate between trees, shrubs, and grass because of their similar spectral characteristics [22,40]. Using multi-temporal NDVI integrated with phenological information on vegetation covers is effectively helpful in differentiating vegetation cover [27,31,32]. Regarding this characteristic, NDVI has been widely used in fire susceptibility studies to represent vegetation dynamics and conditions [40–42].

This research introduces a novel index, the Zagros Grass Index (ZGI) [48]. The ZGI was developed utilizing the Moderate Resolution Imaging Spectroradiometer (MODIS) NDVI to identify dry grass masses highly susceptible to fires. This was achieved by integrating the phenological traits of forest trees and grass species found in Marivan and Sarvabad, located in the western part of Iran. The primary aim of the ZGI is to serve as an easily accessible supplemental tool for detecting and mapping dry grass mass. Designed as an accessible tool for mapping dry grass, the ZGI's utility is further explored in this study by extending the analysis across the Zagros Mountains forests in western Iran and northeastern Iraq from 2013 to 2022. The goal is to assess the ZGI's applicability, scalability, and generalizability to broader areas, enhancing fire management strategies in these regions.

2. Materials and Methods

2.1. The Study Area

The study area is a part of the Kordu–Zagrosian (KZ) forests of Irn and Iraq (longitude: 46°27′37″ E−46°52′20″ E; and latitude: 34°30′55″ N–36°33′5.827″ N), in the northern Zagros Mountain chain with a mean elevation of 1287 m Above Mean Sea Level (AMSL) (Figure 1). Some studies have used the KZ region. It corresponds to a geographical and ecological zone encompassing parts of the Zagros Mountain range across western Iran, eastern Iraq, and southeastern Turkey [49,50].

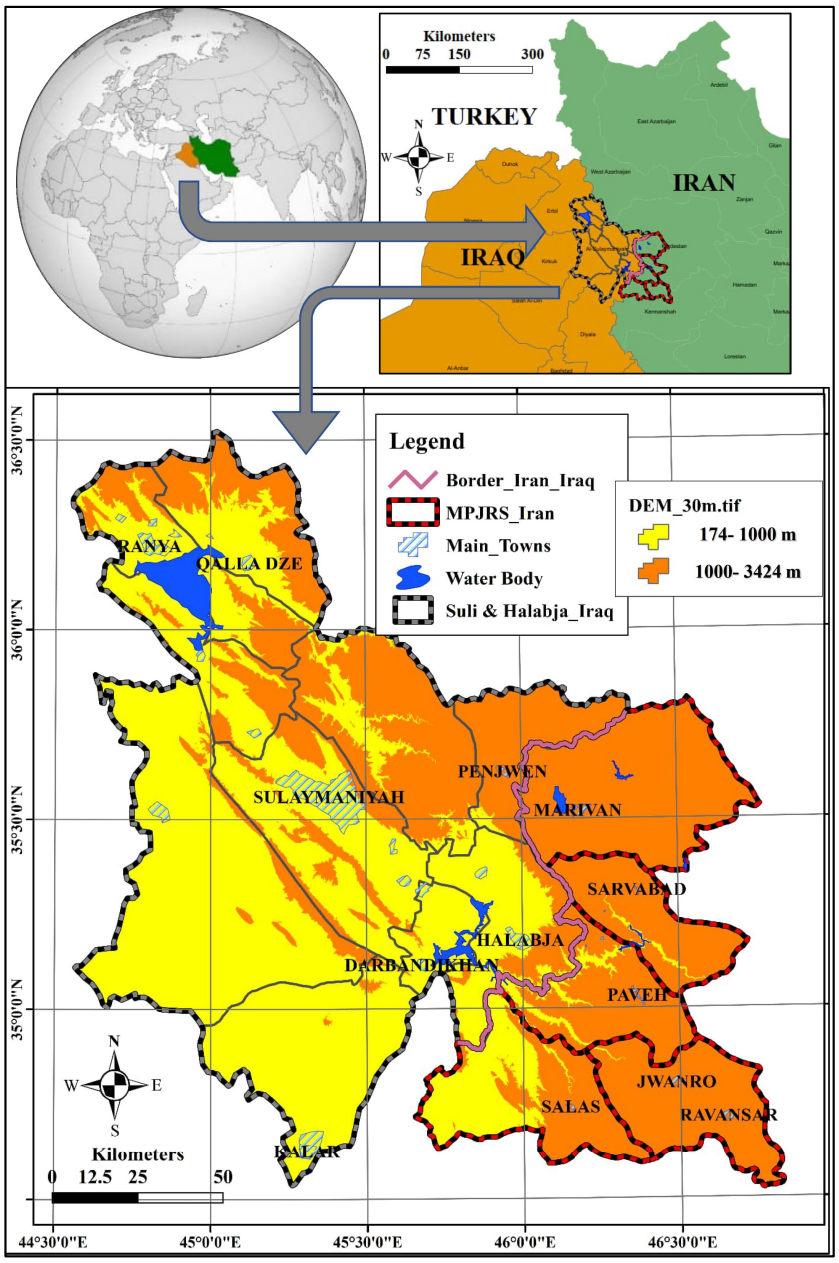


Figure 1. Study Area. Marivan, Sarvabad, Paveh, Jwanro, Ravansar, and Salas in western Iran. Sulaymaniyah Province is in KR, northeast of Iraq.

In Iran, the study area encompasses the forests of Marivan and Sarvabad in Kurdistan Province, as well as Paveh, Javanrod, Ravansar, and Salas in Kermanshah Province, which are in the west of Iran (Figure 1). The study area also covers the vast area of Sulaymaniyah and Halabja provinces in KR, northern Iraq. Most of the Iranian part of the study area (almost 90%) is located below 1000 m AMSL, while nearly 35% of the Iraq study area is higher than 1000 m AMSL, and the rest ranges from almost 200 m to 1000 m AMSL. The KZ forests are dominantly covered by Brant's oaks (Quercus brantii) species in coppice and thin trunks [51], which resulted in the proximity of trees, canopy, and grass species (Figure 2). These forests are also primarily open canopy, expanding mainly between 750 m and 1700 m AMSL [49]. On the other hand, Grass Species (GS), the most vulnerable and flammable fuel type [48,52], extend all over the forests but in different densities, types, and growth patterns. The majority of these species dry in early summer (Figure 2) [10], except for a primarily occurring few species (sub-alpine vegetation), which are mainly in very

high elevations (over 2000 m AMSL) [49] where trees do not grow and forest fires have not occurred there.

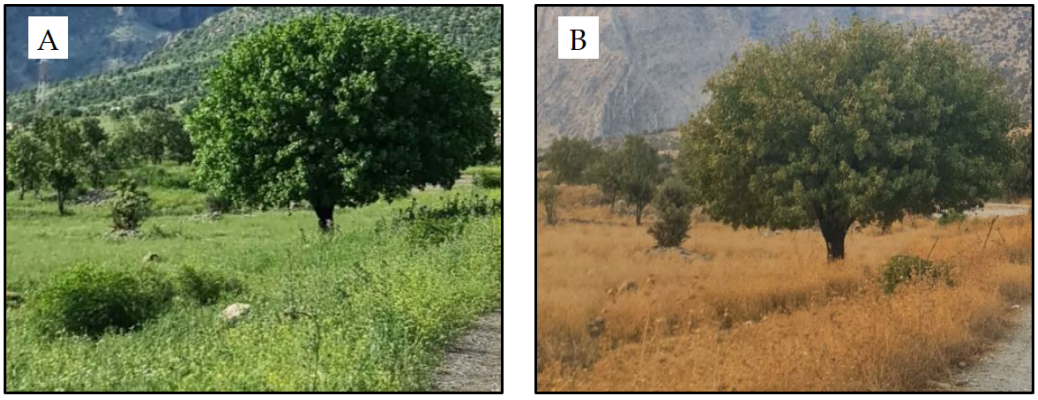


Figure 2. The general structures of KZ forests in spring (**A**) and summer (**B**). While the tree canopy remains green, grasses dry during the summer. Grass and tree canopy are also mixed in KZ forests.

According to official reports, the annual rainfall of Sulaymaniyah and Halabja ranges between 375 and 724 mm, with a semi-arid continental weather regime. It means it is cold and wet in winter and hot and dry in summer [53]. Significantly, the summer months from June to September are very hot and dry, except for the mountainous areas (for example, Hawraman, Qandil, Penjwen, etc.). In July and August, the hottest months, mean temperatures are 39–43 °C and often reach nearly 50 °C [54]. The eastern part of the study area in Iran has more rainfall, with a mean annual precipitation of 700–991 mm and a standard deviation of 200 mm [55].

2.2. Data Sources

In this study, we employed two datasets, satellite imagery and field data, to examine vegetation dynamics (Table 1).

Table 1. Data sources include satellite and field data.

Data	Data Type	Projection	Spatial Resolution (m)	Period	Resource
Satellite Data	MODIS/MOD13Q1	Sinusoidal	250	1 January 2013–31 December 2022	USGS [4]
	DEM [1]/SRTM [2]	UTM [3]	30	-	USGS
In situ Data	Fire statistics	UTM	-	2013–2022	Officials
	Shapefiles (water body, Iran and Iraq national and subnational layers)	UTM	-	-	Officials Report

[1]. Digital Elevation Model. [2]. Shuttle Radar Topography Mission's Digital Elevation Model. [3]. Universal Transverse Mercator. [4]. The United States Geological Survey.

The primary satellite dataset used in this work was the 250 m MODIS vegetation product (MOD13Q1) 16-day time series, covering the period between 2013 and 2022. These data provided access to a broader period regarding our study dataset, while other satellite images (for example, 10 m Sentinel-2 images) cannot offer it despite their higher spatial resolution. Furthermore, the Shuttle Radar Topography Mission's Digital Elevation Model (SRTM DEM) was also used [56]. The SRTM DEM is free to download and provides a spatial resolution of 30 m [56]. The second dataset, provided by the Department of Natural Resources and Watershed (DNRWK) of Kurdistan and Kermanshah Provinces, offers in situ information on fire incidents [57]. Other data, such as the border of the study area,

towns, water bodies, and cultivated areas, were provided by the municipalities of the targeted areas.

2.3. Zagros Grass Index

In this study, we aim to employ our previously established methodology [48] to detect and recognize grass-covered surfaces, a primary fuel source for fires, in the expanded study areas referred to as Kurdo–Zagrosian Forests (KZF). Expanding our methodology, we also refine the proposed index regarding the elevation of the different parts of the study area, considering the effect of elevation on vegetation phenology. Distinct spectral reflectance emitted by vegetation throughout different seasons is effectively characterized by phenological metrics such as the Start of Season (SOS), End of Season (EOS), and Maximum of the Season (MAX) [58]. Figure 3 presents the flowchart that is followed to create ZGI maps. In this context, RS-based VIs, particularly the NDVI, have proven valuable tools for vegetation detection and the extraction of phenological metrics [59]. Historically, the MODIS and the Advanced Very High-Resolution Radiometer (AVHRR) products have been extensively used for estimating these phenological metrics [59–62]. The SRTM DEM was additionally employed to delineate the study area based on elevation, as it significantly influences the phenology of both tree and grass species.

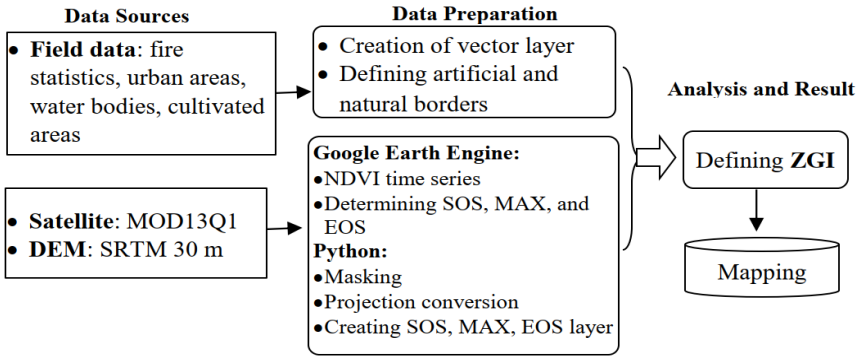


Figure 3. Methodological framework.

Consequently, the elevation affects tree and grass species' SOS, MAX, and EOS [63,64]. Accordingly, the study area was classified into two major classes: (i) the area over 1000 m AMSL and (ii) the area under 1000 m AMSL. Figure 4 illustrates the variation in NDVI changes between areas above 1000 m AMSL and those below 1000 m AMSL.

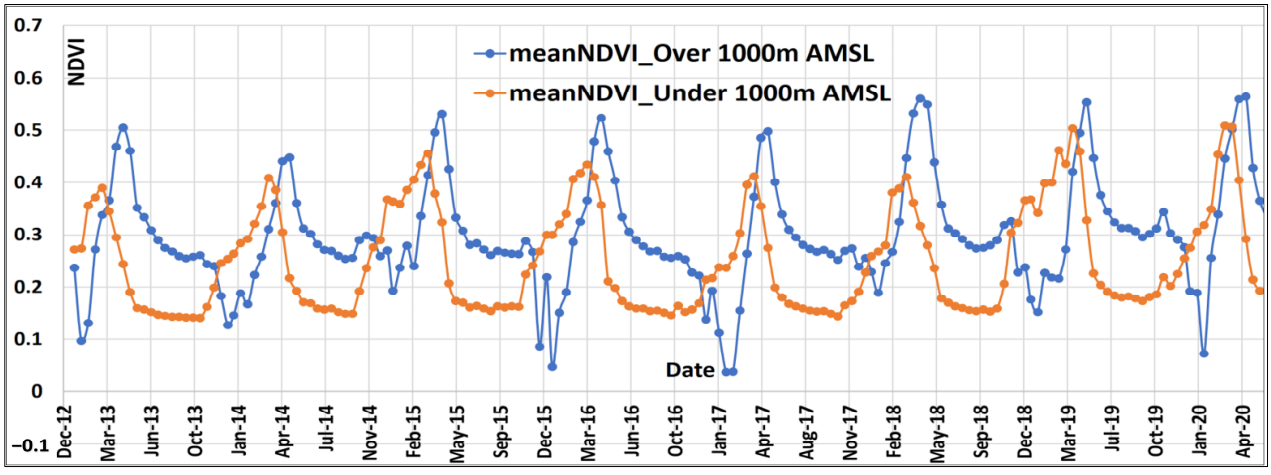


Figure 4. Annual changes of the MODIS Mean NDVI for the areas over and under 1000 m AMSL from 2013 to 2020.

Accordingly, MAX and EOS differ for these two classes, which happen sooner in the lower areas (almost 15 days). Furthermore, the NDVI range for these two classes is different, and the overall NDVI is higher for the area over 1000 m AMSL due to the higher volume of forest area in this area, while the area under 1000 m AMSL is mostly rangelands.

Apart from the effect of elevation on phenological metrics, the tree and grass species in both elevation regions have different phenological behaviors. Figure 5 depicts the overall NDVI changes over time in KZF for either forest area, encompassing both species and rangeland, predominantly covered by grass species.

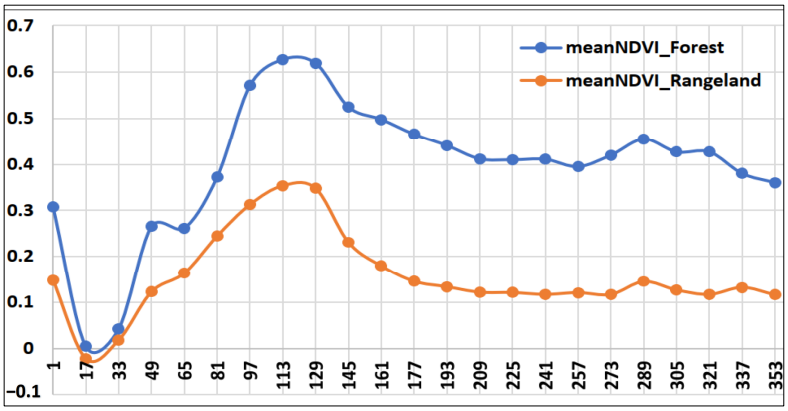


Figure 5. Daily changes of the MODIS mean NDVI during a year for the forest area and rangelands. The forest areas include both species, while rangelands are mostly grass-covered.

Regarding the dependency of phenological metrics on both elevation and vegetation species, the proposed phenological scenario is illustrated in Figure 6.

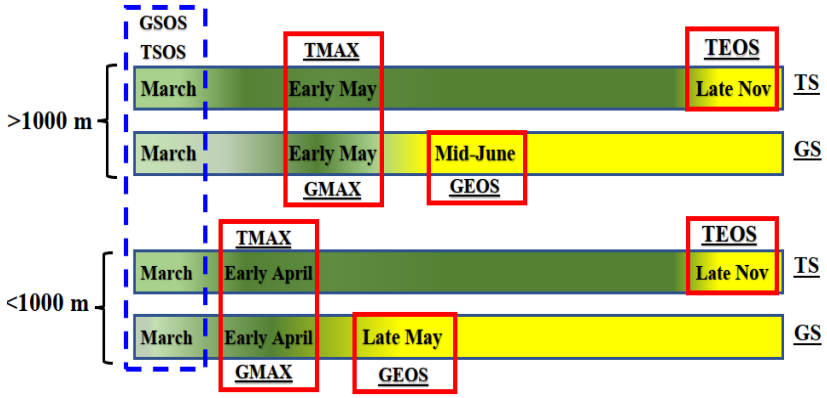


Figure 6. Phenology of the tree and grass species. The blue and red boxes show the incidences of phenological metrics. The SOS for the both species and both elevation ranges happens in March that is displayed within the blue box. The red boxes show other dates within the TMAX, GMAX, GEOS, TEOS, happen.

Accordingly, Grass-SOS (GSOS) and Tree-SOS (TSOS) are almost the same for both elevation ranges, while Grass-MAX (GMAX) and Tree-MAX (TMAX) for higher elevation areas are later than lower elevation areas. Conversely, the EOS differs from trees to grass or from higher to lower areas. Grass-EOS (GEOS) starts in mid-June for higher areas and begins in late May for lower regions. Tree-EOS (TEOS) is almost the same for both elevation ranges. The SOS and EOS do not affect our subject.

According to the phenological scenario (Figure 6), there are life and green Tree Species (TS) and dry and dead Grass Species (GS) after mid-June. Therefore, the greenness after June is only from TS. Consequently, the positive NDVI values that display

green areas are only from TS, and the NDVI values from grass species are almost zero since they have dried.

From a mathematical perspective, the subtraction of GESO's NDVI from GMAX's NDVI can effectively emphasize the presence of grass. This subtraction delineates the decline in NDVI from the TMAX and GMAX to the GEOS, elucidating the extent of grass coverage. It is important to note that this decline solely pertains to non-TS, as the trees retain their greenness. Accordingly, the proposed index is defined in Equations (1) and (2).

For open forest area in each year:

$$ZGI^{open} = NDVI^{GMAX} - NDVI^{GEOS} \quad (1)$$

For dense forest areas in each year:

$$ZGI^{dense} = \text{Average value of } ZGI^{open} = \frac{1}{N}\sum_{n=1}^{N} ZGI_n^{open} \quad (2)$$

where $NDVI^{GMAX}$ corresponds to the NDVI value of the GMAX, which is the date within the NDVI that gives the maximum value due to the attendance of both TS and GS. $NDVI^{GEOS}$ corresponds to the NDVI of the GEOS, which corresponds to the date within the NDVI and gives its minimum value while the TS are still green but the GS has dried [50]. ZGI^{open} is the ZGI of open forests, and ZGI^{dense} is the ZGI of dense forest pixels, which is calculated by averaging the ZGI of neighboring open forest pixels. N is the number of all pixels recognized as open forests each year, and n is the pixel counter.

The ZGI was applied to verified natural surfaces (forests and rangelands) using a designated mask, which excluded the artificial areas (urban, water bodies, rural, and cultivated regions) from the study area. The mask was created from pre-provided maps prepared by DNRWK and then updated manually using QGIS version 3.24.3 software-based maps. Artificial areas are named non-forest areas and represented as black areas in the resulting maps. The areas affected by the fires have been maximized and repositioned within the margins of the maps to better represent the ZGI status in the burned areas and their surrounding regions.

2.4. In Situ Information and Validation

The data on the areas where fires occurred from 2013 to 2022 were used to test the performance of the ZGI. To validate the performance of ZGI, a 500 m buffer has been applied to the fire locations for each year. Then, the buffer polygons were converted to a mask that was applied to the ZGI maps to extract the areas within 500 m away from recorded fire locations. The abundance of each ZGI threshold was calculated to see the distribution of ZGI within the fire areas and their neighborhoods.

3. Results

Regarding the phenological characteristics of the study area (Figure 5), the GMAX is the 129th day for areas over 1000 m and the 113th day for areas under 1000 m AMSL. GEOS is the 257th day of the year in this study. It can also be any other date after mid-June and before early October. The procedural steps resulted in distinct ZGI maps for each year (Figure 7), with the fire occurrence locations provided by the administration of the forest and watershed of Sulaymaniyah, Iraq, and from Kurdistan and Kermanshah provinces in Iran. Most of the data do not encompass the exact locations of fire incidences. Still, rough information on affected areas has been provided, except for Marivan's data, which include a coarse Universal Transverse Mercator (UTM) coordinate (E, N) of fire occurrences. The black areas on the maps denote artificial regions. Several reported fires in agriculture fields are observable within non-forested regions (Figure 8e).

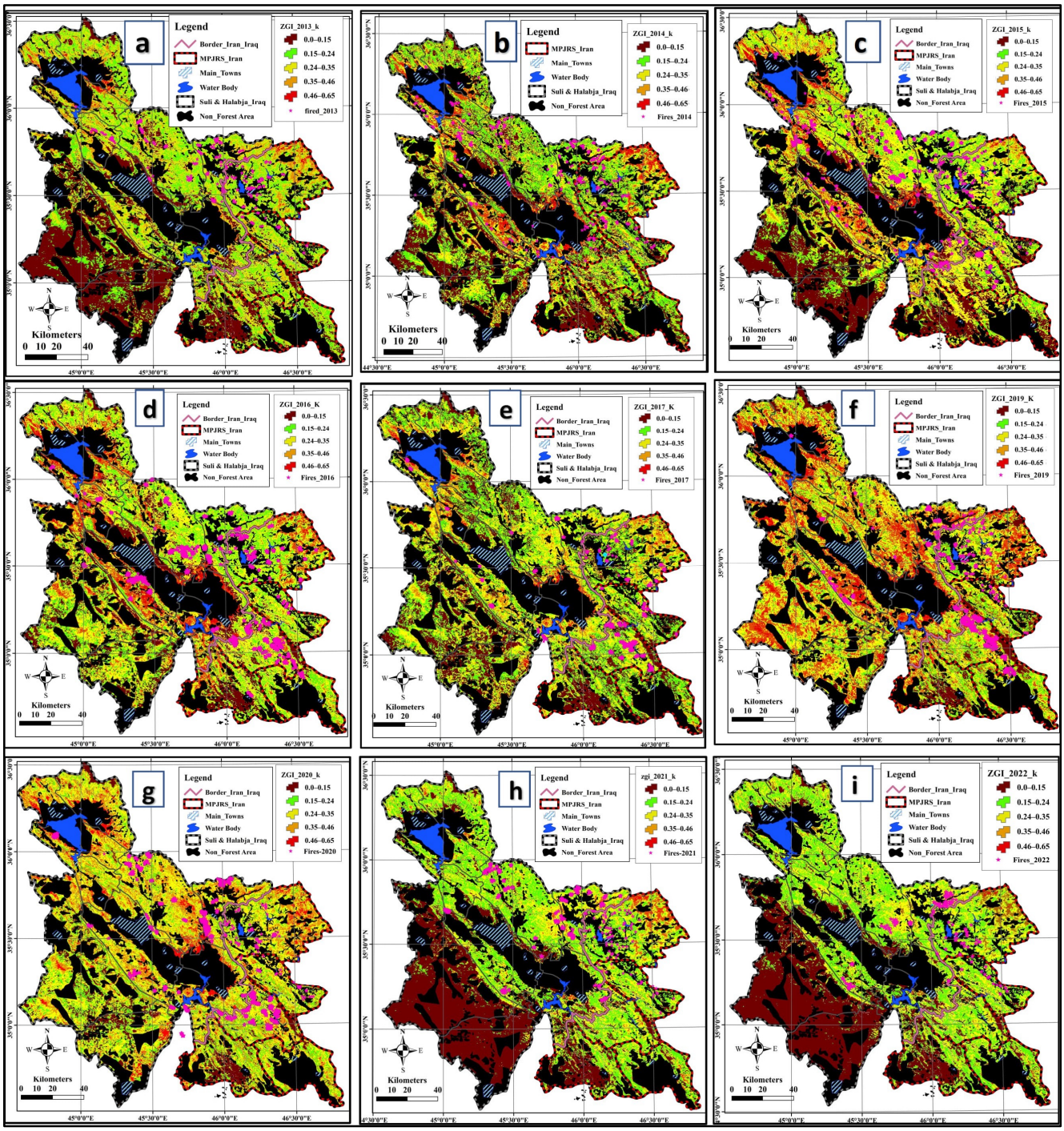


Figure 7. ZGI maps for the years (**a**) 2013; (**b**) 2014; (**c**) 2015; (**d**) 2016; (**e**) 2017; (**f**) 2019; (**g**) 2020; (**h**) 2021; and (**i**) 2022. The purple stars on the maps are the location of the fire, which is presented in purple circles in marginally zoomed subareas. They are labeled using digits so that background information can be observed. The black area represents a non-forested area.

Figure 8 shows the masked areas from 2013 to 2022. Figure 9 shows the annual abundance of ZGI ranges per year in percent. It also shows the cumulative abundance for ZGI > 0.15 and ZGI > 0.24. More than 90% of pixels within 500 m around the fire areas belong to class ZGI > 0.15, and more than 68% belong to class ZGI > 0.24. Based on the statistical report (following Figure 9), the majority of fire areas belong to the range of 0.15 < ZGI < 0.46.

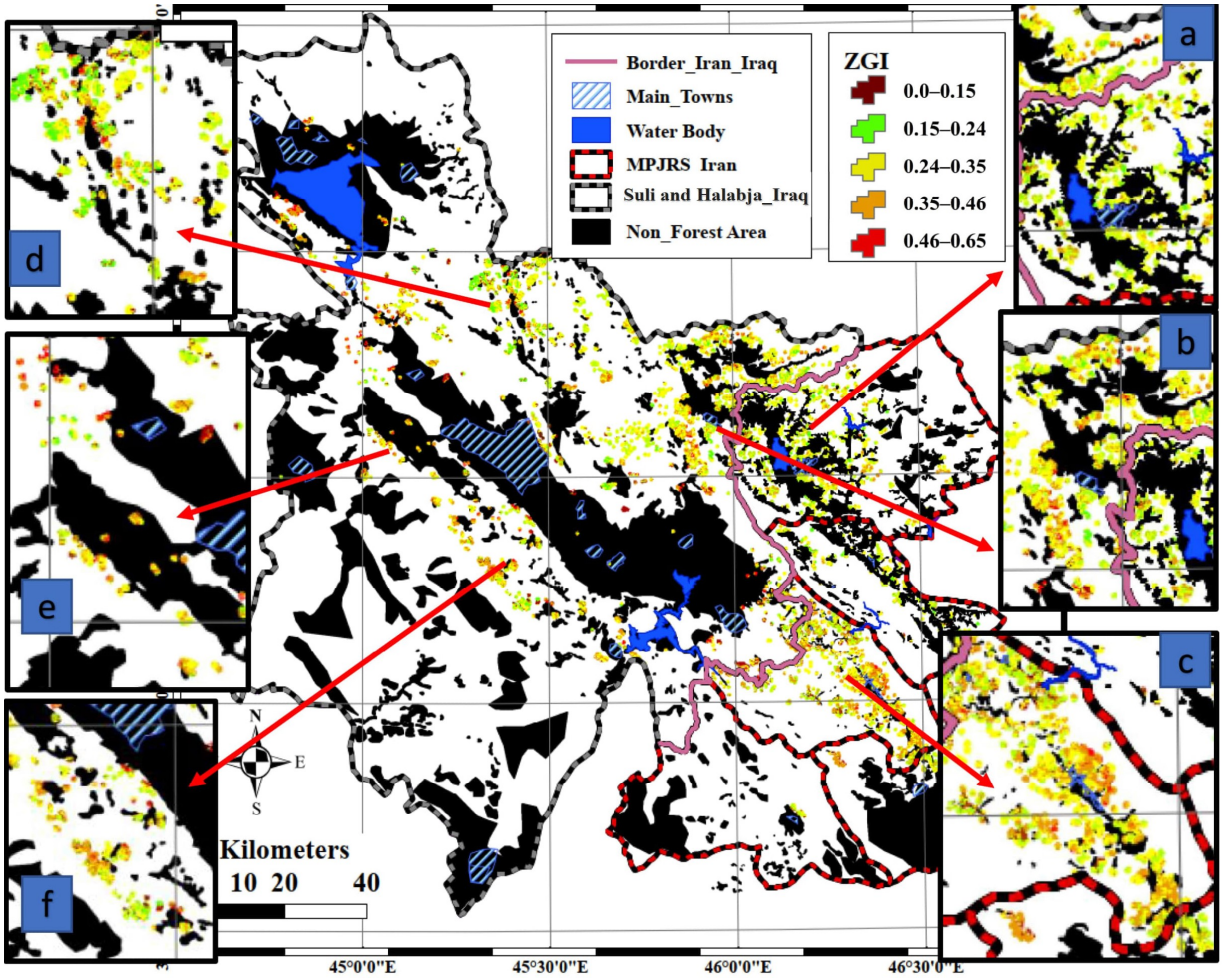


Figure 8. Masked ZGI within the 500 m buffer around the fire locations from 2013–2022. Black areas are non-forest areas. The subfigures (**a**–**f**), display some parts of the study area with high wildfire experiences in a more visible view.

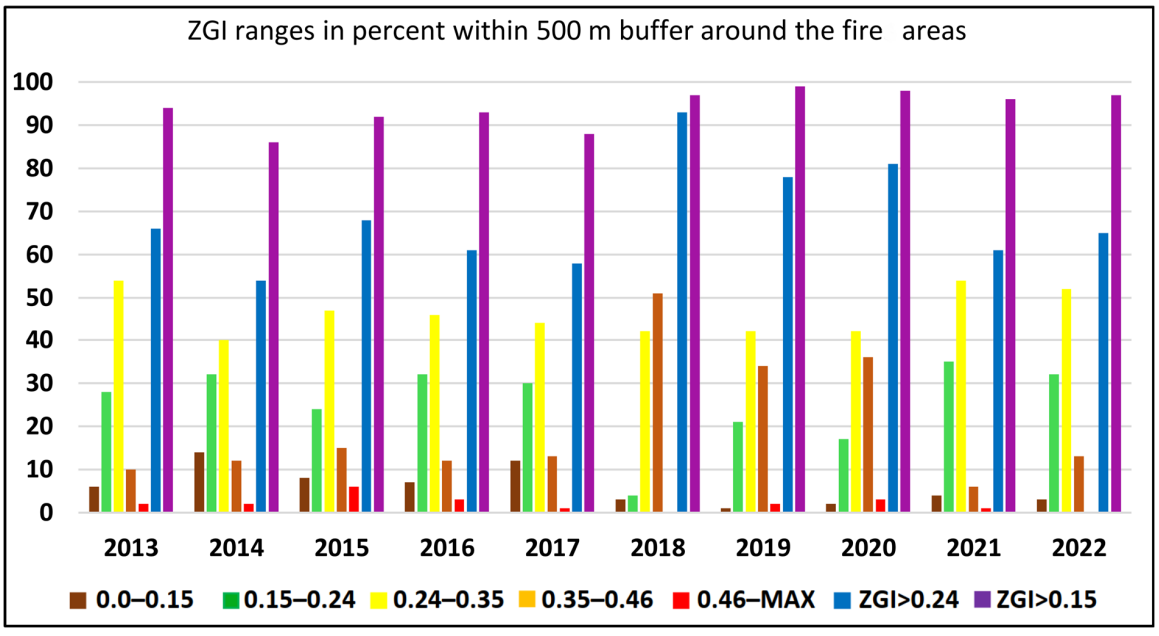


Figure 9. The annual abundance of ZGI ranges per year and the cumulative abundance for ZGI > 0.15 and ZGI > 0.24.

4. Discussion

The resulting maps revealed distinct patterns in the ZGI for each year, consistent with previous studies, that underscore the significant influence of climate conditions, such as rainfall and temperature, on the vegetation cover in semi-arid and semi-Mediterranean regions [30,34,65,66]. The ZGI thresholds have been defined using the Natural Breaks (NB) method, which is based on actual values in the dataset rather than using predefined intervals [43]. Since the fires are primarily human-caused [13,14], deliberately or accidentally, the affected areas are majorly adjacent to the artificial regions where humans are living or cultivating areas where humans live or cultivate [40,67]. Despite the remarkable results of previous studies on land cover mapping within the study area and regions with comparable climate conditions, particularly emphasizing grass species as ecological contributors [22–39], this study focuses on grass as a potential source of dangerous dead biomass and the most flammable fuel type in our study area and other similar regions [40–42]. The spread and continuity of dead or living vegetation are primary factors in sustaining fires, and dry grasses—especially dense ones—have been proven to have the highest potential for fire propagation [40,68,69]. Consequently, identifying and mapping fuel types is crucial in defining risk conditions [41]. Fuel models involve the parameterization of different fuel types to estimate their fire behavior [38,70]. Various methodologies have been developed to generate and map fuel types according to the input data, intended use, and scale of the study [20,40,68,69,71]. Despite numerous global studies characterizing different fuel types through detailed parameters such as crown height, crown base height, vegetation coverage percentage, forest canopy density, crown density, canopy bulk density, number of trees per area, vertical and horizontal continuity, moisture content, live and dead fuel load, biomass [71], and using RS data/methods, this study focuses on dry grass mass [41,68]. It leverages the phenological characteristics of grass and woody species within the study area. Furthermore, the KZ's coppiced TS are more susceptible to ignition by fires originating from grasses than conifers (for example, pines) and other TS, which have been addressed and categorized in other studies [41,51].

The resulting maps prove that the fires strongly overlap and follow the areas with higher ZGI values, precisely $0.24 < ZGI < 0.35$ and $0.35 < ZGI < 0.46$. The higher ZGI range ($ZGI > 0.46$) belongs to mountainous areas (over 2000 m AMSL), covered mainly by sub-alpine vegetation species, and rarely experiences fire [50]. As seen, more than 90% of pixels within 500 m around the fire areas belong to $ZGI > 0.15$, and more than 68% of pixels belong to $ZGI > 0.24$. Based on the statistical report, most fire areas belong to the range $0.15 < ZGI < 0.46$. Although, in some years with lower overall ZGI values, lower fires have been reported (for example, Figure 7a,h,i), it cannot be inferred that poorer dry grass mass necessarily results in less fire, as seen in Figure 7c, since the overall ZGI does not mean that dry grass mass is necessarily low all over the study area. Another reason is the coppice structures of most forest trees, which make them vulnerable even against fires ignited by poor grass conditions (Figure 2) [72]. The severity of fires should also be considered to provide a more comprehensive understanding of fire behavior. Reliable information on dry grass mass in fire season (late May–late October) can also provide a reliable view of the fire's propagation rate and severity [40,68]. Although the fire severity and propagation rate have not been addressed directly in this study, ZGI can also help us with those because it can be inferred that the severity and propagation of fires could be potentially very high among dense forests with highly flammable grass masses (high ZGI values) [40,68]. Moreover, it is imperative to consider the various grass species, considering their distinct phenology, density, propagation, ignitability, power of ignition, and firing duration.

The maps further indicate that within areas above 1000 m AMSL, the ZGI values are higher than those in lower elevations [10,30,33,34]. This observation aligns with the overall fire distribution across the study area, as depicted in Figure 7, affirming that the fire tends to be higher in regions above 1000 m AMSL. It is also observed from the maps that the areas close to human-associated areas (black areas) with lower ZGI (brown and green areas) have rarely been subjected to fires. Therefore, the integration of human accessibility and

ZGI, rather than higher ZGI values alone, emerges as a significant factor in fire incidences. Comparing the frequent application of NDVI and fire susceptibility as a vegetation detector in Zagros forests [10,30,33,34,40], ZGI also seems to be a suitable index for the study area since it targets the dry mass through pixel-wise temporal change detection of NDVI regarding the phenological characteristics of the grass and non-grass covers.

In fire susceptibility mapping, various vegetation indices are employed to assess the likelihood of fire occurrence and vegetation vulnerability. The NDVI measures vegetation health and density, while the Enhanced Vegetation Index (EVI) offers improved sensitivity to canopy structural variations. The Normalized Burn Ratio (NBR) aids in identifying burn severity and post-fire vegetation recovery, while the Soil Adjusted Vegetation Index (SAVI) accounts for soil reflectance variations. The Fire Risk Index (FRI) combines multiple indices and environmental factors to evaluate fire risk comprehensively. However, a comparison with a novel index derived from subtracting maximum NDVI in spring from the end-of-season NDVI of grass species in summer is warranted to enhance fire susceptibility assessment further. Given the unique seasonal dynamics captured by this novel approach and its potential to provide valuable insights into vegetation-fire relationships, conducting a comparative study with existing indices would require an independent investigation in the future. Such a study could refine fire susceptibility mapping methodologies and improve our understanding of wildfire dynamics in diverse ecosystems. The Zagros Forest region experiences a semi-Mediterranean and continental semi-arid climate regime characterized by hot, dry summers and mild, wet winters [71], regarding the vast distribution of this type of climate regime. This index can be generalized and used in other study areas, for example, California (USA), the Mediterranean Basin, and southwestern Australia [72].

5. Conclusions

These forest structures and the composition of grass species, in conjunction with human activities, emerge as significant contributors to the incidence of wildfires. Effectively mapping grass species enhances our comprehension of fire susceptibility, its duration, and spatial distribution. Integrating RS data/techniques with GIS expedites a precise analysis of wildfire dynamics, providing reliable insights into vegetation species' dynamic and static conditions. Moreover, phenological characteristics can be harnessed to formulate novel RS indices, as exemplified by the ZGI applied in this study. The resulting maps exhibit a pronounced overlap between ZGI and areas accessible to human activities, suggesting a notable correlation between human-caused fires and regions with high ZGI values. The ZGI can be used jointly with other VIs (for example, NDVI) or as an alternative index for providing helpful vegetation dynamic, flammable area, and fuel load among, NDVI) or as an alternative index for providing helpful vegetation dynamic, flammable area, and fuel load among the Zagros Mountains in Iran and Iraq.

Regarding the coarse resolution of MODIS images, the ZGI is only based on the overall phenological and spectral characteristics of trees and grass covers, ignoring texture differences, unlike urban areas utilizing high-resolution images. Therefore, future research may benefit from using satellite images with a higher spatial resolution (for example, Sentinel-2, Landsat-8/9, and GeoEye) for enhanced accuracy. The pursuit of further studies using satellite imagery with higher spatial resolution can yield more reliable results, offering improved insights into fire dynamics and vegetation characteristics at finer scales. The higher ZGI value, consequently, shows a drier mass. Nevertheless, this criterion alone is insufficient for predicting fires; multiple other factors (for example, temperature, aspect, slope, distance from the population center and road, etc.) must be considered contributors to fire susceptibility.

However, this study needs more precise details, such as the coordinate system, areas affected, fire types, and causes. Some years did not have corresponding data on fires as well. For example, we did not access any recorded data related to the years before 2015 or 2021 for Kermanshah province cities (Paveh, Jwanro, Ravansar, and Salas). We also could not find any data about the Marivan and Sarvabad fires in 2018. Lack of awareness

or attention from relevant administrations in obtaining accurate data on fire incidences, including field observations on fire severity, a dependable map of burned areas, and precise ignition points, has complicated the execution of our study. Regarding the study area's semi-Mediterranean and continental semi-arid climate, characterized by hot, dry summers and mild, wet winters, this index can be generalized to other study areas, for example, California (USA), the Mediterranean Basin, and Southwestern Australia.

In this paper, we have studied the use of the Zagros Grass Index in fire assessment within the Zagros Mountains. This research is vital for disaster reduction and fire prevention, which are essential for sustainable development. Taking proactive measures to prevent fires and mitigate disaster risks can promote resilience, conserve resources, protect lives and property, and contribute to long-term sustainability efforts.

Author Contributions: Conceptualization, I.R.; methodology, I.R.; software, I.R.; investigation, I.R. and L.D.; data curation, I.R.; writing—original draft preparation, I.R.; writing—review and editing, I.R., L.D. and A.C.T.; funding acquisition, A.C.T. and L.D. All authors have read and agreed to the published version of the manuscript.

Funding: This research received no external funding.

Institutional Review Board Statement: Not applicable.

Informed Consent Statement: Not applicable.

Data Availability Statement: The original contributions presented in the study are included in the article, further inquiries can be directed to the corresponding author.

Acknowledgments: This work is supported by national funding awarded by FCT—Foundation for Science and Tech-nology, I.P., projects UIDB/04683/2020 (https://doi.org/10.54499/UIDB/04683/2020) and UIDP/04683/2020 (https://doi.org/10.54499/UIDP/04683/2020).

Conflicts of Interest: The authors declare no conflict of interest.

References

1. Bajocco, S.; Rosati, L.; Ricotta, C. Knowing fire incidence through fuel phenology: A remotely sensed approach. *Ecol. Model.* **2010**, *221*, 59–66. [CrossRef]
2. Pacheco, A.P.; Claro, J.; Fernandes, P.M.; De Neufville, R.; Oliveira, T.; Borges, J.G.; Rodrigues, J. Cohesive fire management within an uncertain environment: A review of risk handling and decision support systems. *For. Ecol. Manag.* **2015**, *347*, 1–17. [CrossRef]
3. Pourtaghi, Z.S.; Pourghasemi, H.R.; Aretano, R.; Semeraro, T. Investigation of general indicators influencing on forest fire and its susceptibility modeling using different data mining techniques. *Ecol. Indic.* **2016**, *64*, 72–84. [CrossRef]
4. Levine, J.S. *Global Biomass Burning*; MIT Press eBooks: Cambridge, MA, USA, 1991. [CrossRef]
5. Cao, Y.; Wang, M.; Li, K. Wildfire susceptibility assessment in Southern China: A comparison of multiple methods. *Int. J. Disaster Risk Sci.* **2017**, *8*, 164–181. [CrossRef]
6. Carlson, J.D.; Burgan, R.E. Review of users' needs in operational fire danger estimation: The Oklahoma example. *Int. J. Remote Sens.* **2003**, *24*, 1601–1620. [CrossRef]
7. Fernández-Guisuraga, J.M.; Suárez-Seoane, S.; Calvo, L. Radiative transfer modeling to measure fire impact and forest engineering resilience at short-term. *Isprs J. Photogramm. Remote Sens.* **2021**, *176*, 30–41. [CrossRef]
8. Shaluf, I.M. Technological disaster stages and management. *Disaster Prev. Manag.* **2008**, *17*, 114–126. [CrossRef]
9. Oliveira, S.; Laneve, G.; Fusilli, L.; GeorgiosEftychidis Nunes, A.; Lourenço, L.; López, A.S. *A Common Approach to Foster Prevention and Recovery of Forest Fires in Mediterranean Europe*; InTech eBooks: London, UK, 2017. [CrossRef]
10. Rahimi, I.; Azeez, S.N.; Ahmed, I.H. *Mapping Forest-Fire Potentiality Using Remote Sensing and GIS, Case Study: Kurdistan Region-Iraq*; Springer Water: Berlin/Heidelberg, Germany, 2019; pp. 499–513. [CrossRef]
11. Tian, X.; Zhao, F.; Shu, L.; Wang, M. Distribution characteristics and the influence factors of forest fires in China. *For. Ecol. Manag.* **2013**, *310*, 460–467. [CrossRef]
12. Adab, H.; Kanniah, K.D.; Solaimani, K.; Sallehuddin, R. Modelling static fire hazard in a semi-arid region using frequency analysis. *Int. J. Wildland Fire* **2015**, *24*, 763. [CrossRef]
13. Causes of Fire Incidences in Kurdistan Forests. ISNA. Available online: https://www.isna.ir/xd54pZ (accessed on 10 August 2019).
14. Rojhelat Environmentalists Blame Government Inactivity for Frequent Forest Fires. RUDAW. Available online: https://www.rudaw.net (accessed on 17 August 2023).
15. San-Miguel-Ayanz, J.; Durrant, T.; Boca, R.; Maianti, P.; Liberta', G.; Artes, V.T.; Jacome, F.O.D.; Branco, A.; De, R.D.; Ferrari, D.; et al. Advance report on wildfires in Europe, Middle East and North Africa 2021. *JRC Publ. Repos.* 2021. [CrossRef]

16. *Press Corner. (n.d.). European Commission—European Commission*. Available online: https://ec.europa.eu/commission/presscorner/detail/en/IP_23_5951 (accessed on 22 November 2023).
17. Teodoro, A.C.; Santos, P.; Marques, J.E.; Ribeiro, J.; Mansilha, C.; Melo, A.; Duarte, L.; De Almeida, C.R.; Flores, D. An Integrated Multi-Approach to Environmental Monitoring of a Self-Burning Coal Waste Pile: The São Pedro da Cova Mine (Porto, Portugal) Study Case. *Environments* **2021**, *8*, 48. [CrossRef]
18. Teodoro, A.C.; Amaral, A.L. A statistical and spatial analysis of Portuguese forest fires in summer 2016 considering Landsat 8 and Sentinel 2A data. *Environments* **2019**, *6*, 36. [CrossRef]
19. Teodoro, A.C.; Duarte, L. Forest fire risk maps: A GIS open source application—A case study in Norwest of Portugal. *Int. J. Geogr. Inf. Sci.* **2013**, *27*, 699–720. [CrossRef]
20. Dasgupta, S.; Qu, J.J.; Hao, X.; Bhoi, S. Evaluating remotely sensed live fuel moisture estimations for fire behavior predictions in Georgia, USA. *Remote Sens. Environ.* **2007**, *108*, 138–150. [CrossRef]
21. Babu, K.V.S.; Vanama, V.S.K.; Roy, A.; Prasad, P. Assessment of forest fire danger using automatic weather stations and MODIS TERRA satellite datasets for the state Madhya Pradesh, India. In Proceedings of the 2017 International Conference on Advances in Computing, Communications and Informatics (ICACCI), Udupi, India, 13–16 September 2017; IEEE: Piscataway, NJ, USA, 2017. [CrossRef]
22. Saah, D.; Tenneson, K.; Matin, M.A.; Uddin, K.; Cutter, P.; Poortinga, A.; Nguyen, Q.; Patterson, M.; Johnson, G.W.; Markert, K.; et al. Land cover mapping in data scarce Environments: Challenges and opportunities. *Front. Environ. Sci.* **2019**, *7*, 150. [CrossRef]
23. Hellesen, T.; Matikainen, L. An Object-Based approach for mapping shrub and tree cover on grassland habitats by use of LIDAR and CIR orthoimages. *Remote Sens.* **2013**, *5*, 558–583. [CrossRef]
24. Guirado, E.; Tabik, S.; Alcaraz-Segura, D.; Cabello, J.; Herrera, F. Deep-learning Versus OBIA for Scattered Shrub Detection with Google Earth Imagery: Ziziphus lotus as Case Study. *Remote Sens.* **2017**, *9*, 1220. [CrossRef]
25. Ayhan, B.; Kwan, C. Tree, shrub, and grass classification using only RGB images. *Remote Sens* **2020**, *12*, 1333. [CrossRef]
26. Zaabar, N.; Niculescu, S.; Mihoubi, M.K. Application of convolutional neural networks with Object-Based image analysis for land cover and land use mapping in coastal areas: A case study in Ain Témouchent, Algeria. *IEEE J. Sel. Top. Appl. Earth Obs. Remote Sens.* **2022**, *15*, 5177–5189. [CrossRef]
27. Madasa, A.; Orimoloye, I.R.; Ololade, O.O. Application of geospatial indices for mapping land cover/use change detection in a mining area. *J. Afr. Earth Sci.* **2021**, *175*, 104108. [CrossRef]
28. Diaz, B.M.; Blackburn, G.A. Remote sensing of mangrove biophysical properties: Evidence from a laboratory simulation of the possible effects of background variation on spectral vegetation indices. *Int. J. Remote Sens.* **2003**, *24*, 53–73. [CrossRef]
29. Meshesha, D.T.; Ahmed, M.M.; Abdi, D.Y.; Haregeweyn, N. Prediction of grass biomass from satellite imagery in Somali regional state, eastern Ethiopia. *Heliyon* **2020**, *6*, e05272. [CrossRef] [PubMed]
30. Fakhri, S.A.; Sayadi, S.; Naghavi, H.; Latifi, H. A novel vegetation index-based workflow for semi-arid, sparse woody cover mapping. *J. Arid. Environ.* **2022**, *201*, 104748. [CrossRef]
31. Qian, Y.; Zhou, W.; Nytch, C.J.; Han, L.; Li, Z. A new index to differentiate tree and grass based on high resolution image and object-based methods. *Urban For. Urban Green.* **2020**, *53*, 126661. [CrossRef]
32. Grigorieva, O.V.; Brovkina, O.; Saidov, A. An original method for tree species classification using multitemporal multispectral and hyperspectral satellite data. *Silva Fenn.* **2020**, *54*, 10143. [CrossRef]
33. Eskandari, S.; Jaafari, M.R.; Oliva, P.; Ghorbanzadeh, O.; Blaschke, T. Mapping land cover and tree canopy cover in Zagros forests of Iran: Application of Sentinel-2, Google Earth, and field data. *Remote Sens.* **2020**, *12*, 1912. [CrossRef]
34. Shafeian, E.; Fassnacht, F.E.; Latifi, H. Mapping fractional woody cover in an extensive semi-arid woodland area at different spatial grains with Sentinel-2 and very high-resolution data. *Int. J. Appl. Earth Obs. Geoinf.* **2021**, *105*, 102621. [CrossRef]
35. Nasir, S.M.; Kamran, K.V.; Blaschke, T.; Karimzadeh, S. Change of land use/land cover in kurdistan region of Iraq: A semi-automated object-based approach. *Remote Sens. Appl. Soc. Environ.* **2022**, *26*, 100713. [CrossRef]
36. Rash, A.; Mustafa, Y.T.; Hamad, R. Quantitative assessment of Land use/land cover changes in a developing region using machine learning algorithms: A case study in the Kurdistan Region, Iraq. *Heliyon* **2023**, *9*, e21253. [CrossRef]
37. Aragoneses, E.; Chuvieco, E. Generation and mapping of fuel types for fire risk assessment. *Fire* **2023**, *4*, 59. [CrossRef]
38. Pettinari, M.L.; Chuvieco, E. Fire Behavior Simulation from Global Fuel and Climatic Information. *Forests* **2017**, *8*, 179. [CrossRef]
39. Motlagh, M.G.; Alchin, A.A.; Daghestani, M. Detection of high fire risk areas in Zagros Oak forests using geospatial methods with GIS techniques. *Arab. J. Geosci.* **2022**, *15*, 835. [CrossRef]
40. Taufik, A.; Ahmad, S.S.S.; Ahmad, A. Classification of Landsat 8 satellite data using NDVI tresholds. *J. Telecommun. Electron. Comput. Eng.* **2016**, *8*, 37–40. Available online: https://jtec.utem.edu.my/jtec/article/view/1168 (accessed on 22 November 2023).
41. Pettorelli, N.; Vik, J.O.; Mysterud, A.; Gaillard, J.; Tucker, C.J.; Stenseth, N.C. Using the satellite-derived NDVI to assess ecological responses to environmental change. *Trends Ecol. Evol.* **2005**, *20*, 503–510. [CrossRef] [PubMed]
42. McInnes, W.S.; Smith, B.; McDermid, G.J. Discriminating native and nonnative grasses in the dry mixedgrass prairie with MODIS NDVI Time Series. *IEEE J. Sel. Top. Appl. Earth Obs. Remote Sens.* **2015**, *8*, 1395–1403. [CrossRef]
43. Clementini, C.; Del Frate, F.; Pomente, A.; Salvucci, G.D.; Teillard, F.; Kanamaru, H.; Fujisawa, M.; Mottet, A.; Heureux, A. Grass Biomass Estimation on Zambian pastures for future climate Change Effects Mitigation and adaptation using satellite imagery and neural network technique. In Proceedings of the IGARSS 2018—2018 IEEE International Geoscience and Remote Sensing Symposium, Valencia, Spain, 22–27 July 2018; IEEE: Piscataway, NJ, USA, 2018. [CrossRef]

44. Royimani, L.; Mutanga, O.; Dube, T. Progress in Remote sensing of grass senescence: A review on the challenges and opportunities. *IEEE J. Sel. Top. Appl. Earth Obs. Remote Sens.* **2021**, *14*, 7714–7723. [CrossRef]
45. Rahimi, I.; Duarte, L.; Teodoro, A.C. A new indicator for enhancing fire fuel mapping in Marivan forests, west of Iran. In Proceedings of the SPIE 12734, Earth Resources and Environmental Remote Sensing/GIS Applications, Amsterdam, The Netherlands, 6–9 September 2023. [CrossRef]
46. Abu-Rabia, A. Ethno-Botanic Treatments for Paralysis (FALIJ) in the Middle East. *Chin. Med.* **2012**, *3*, 157–166. [CrossRef]
47. El-Moslimany, A.P. Ecology and late-Quaternary history of the Kurdo-Zagrosian oak forest near Lake Zeribar, western Iran. *Vegetation* **1986**, *68*, 55–63. [CrossRef]
48. Pourhashemi, M.; Zandebasiri, P. Panahi, Structural characteristics of oak coppice stands of Marivan Forests. *Iran. J. Plant Res.* **2014**, *27*, 766–776.
49. Jazirehi, M.H.; Rostaaghi, E.M. *Silviculture in Zagros*; University of Tehran Press: Tehran, Iran; Scientific Research Publishing: Wuhan, China, 2003; 560p. Available online: https://www.scirp.org/reference/referencespapers?referenceid=1852053 (accessed on 20 November 2023).
50. Kurdistan Regional Government. KRG Administered Territory. 2023. Available online: https://gov.krd/english (accessed on 23 November 2023).
51. Kurdistan Region Presidency. Oil-for-Food Distribution Plan. Approved by the UN, December. UNEP. Available online: https://presidency.gov.krd/krp/english/ndisplay.aspx?sm=5yBwBg+oqQY= (accessed on 23 November 2023).
52. Rahimzadeh-Bajgiran, P.; Darvishsefat, A.A.; Khalili, A.; Makhdoum, M. Using AVHRR-based vegetation indices for drought monitoring in the Northwest of Iran. *J. Arid. Environ.* **2008**, *72*, 1086–1096. [CrossRef]
53. USGS EROS Archive—Digital Elevation—Shuttle Radar Topography Mission (SRTM) 1 ArC-Second Global | U.S. Geological Survey. (July 2018). Available online: https://www.usgs.gov/centers/eros/science/usgs-eros-archive-digital-elevation-shuttle-radar-topography-mission-srtm-1 (accessed on 20 November 2023).
54. Kheshti, M. Protect Iran's Zagros forests from wildfires. *Science* **2020**, *369*, 1066. [CrossRef] [PubMed]
55. Duarte, L.; Teodoro, A.C.; Gonçalves, H. Deriving phenological metrics from NDVI through an open source tool developed in QGIS. In Proceedings of the Volume 9245, Earth Resources and Environmental Remote Sensing/GIS Applications V, 924511, Amsterdam, The Netherlands, 23–25 September 2014.
56. Malhi, R.K.M.; Kiran, G.S.; Shah, M.N.; Mistry, N.; Bhavsar, V.H.; Singh, C.P.; Bhattarcharya, B.K.; Townsend, P.A.; Mohan, S. Applicability of Smoothing Techniques in Generation of Phenological Metrics of *Tectona grandis* L. Using NDVI Time Series Data. *Remote Sens.* **2021**, *13*, 3343. [CrossRef]
57. Chen, X.; Xu, C.; Tan, Z. An analysis of relationships among plant community phenology and seasonal metrics of Normalized Difference Vegetation Index in the northern part of the monsoon region of China. *Int. J. Biometeorol.* **2001**, *45*, 170–177. [CrossRef] [PubMed]
58. Hott, M.C.; Carvalho, L.M.T.; Antunes, M.A.H.; Resende, J.C.; Rocha, W.S.D. Analysis of Grassland Degradation in Zona da Mata, MG, Brazil, Based on NDVI Time Series Data with the Integration of Phenological Metrics. *Remote Sens.* **2019**, *11*, 2956. [CrossRef]
59. Ji, Z.; Pan, Y.; Zhu, X.; Wang, J.; Li, Q. Prediction of Crop Yield Using Phenological Information Extracted from Remote Sensing Vegetation Index. *Sensors* **2021**, *21*, 1406. [CrossRef]
60. Li, M.; Bao, G.; Tong, S.; Yin, S.; Bao, Y.; Jiang, K.; Hong, Y.; Tuya, A.; Huang, X. Elevation-dependent response of spring phenology to climate and its legacy effect on vegetation growth in the mountains of northwest Mongolia. *Ecol. Indic.* **2021**, *126*, 107640. [CrossRef]
61. Ziello, C.; Estrella, N.; Kostova, M.; Koch, E.; Menzel, A. Influence of altitude on phenology of selected plant species in the Alpine region (1971–2000). *Clim. Res.* **2009**, *39*, 227–234. Available online: https://www.jstor.org/stable/24870440 (accessed on 10 December 2023). [CrossRef]
62. Yang, J.; Weisberg, P.J.; Bristow, N. Landsat remote sensing approaches for monitoring long-term tree cover dynamics in semi-arid woodlands: Comparison of vegetation indices and spectral mixture analysis. *Remote Sens. Environ.* **2012**, *119*, 62–71. [CrossRef]
63. Higginbottom, T.P.; Symeonakis, E.; Meyer, H.; Van Der Linden, S. Mapping fractional woody cover in semi-arid savannahs using multi-seasonal composites from Landsat data. *Isprs J. Photogramm. Remote Sens.* **2018**, *139*, 88–102. [CrossRef]
64. Yulianto, F.; Kushardono, D.; Budhiman, S.; Nugroho, G.; Chulafak, G.A.; Dewi, E.K.; Pambudi, A.I. Evaluation of the threshold for an improved surface water extraction index using optical remote sensing data. *Sci. World J.* **2022**, *2022*, 4894929. [CrossRef]
65. MosaBeigi, M.; Mirza Beigi, F. Zoning forest fire risk in the Manesht and Qalarang Protected Area using a network analysis model and geographic information system. *Environ. Sci.* **2017**, *14*, 175–188. (In Persian)
66. Zaïdi, A. Predicting wildfires in Algerian forests using machine learning models. *Heliyon* **2023**, *9*, e18064. [CrossRef] [PubMed]
67. Scott, J.R.; Burgan, R.E. Standard fire behavior fuel models: A comprehensive set for use with Rothermel's surface fire spread model. In *General Technical Report*; U.S. Department of Agriculture, Forest Service, Rocky Mountain Research Station: Fort Collins, CO, USA, 2005; 72p. [CrossRef]
68. Wragg, P.D.; Mielke, T.; Tilman, D. Forbs, grasses, and grassland fire behaviour. *J. Ecol.* **2018**, *106*, 1983–2001. [CrossRef]
69. Pourreza, M.; Hosseini, S.M.; Sinegani, A.A.S.; Matinizadeh, M.; Alavai, S.J. Herbaceous species diversity in relation to fire severity in Zagros oak forests, Iran. *J. For. Res.* **2014**, *25*, 113–120. [CrossRef]
70. Chuvieco, E.; Riaño, D.; Van Wagtendonk, J.W.; Morsdof, F. Fuel loads and fuel type mapping. *Ser. Remote Sens.* **2003**, *4*, 119–142. [CrossRef]

71. Sagheb-Talebi, K.; Sajedi, T.; Pourhashemi, M. Forests of Iran. In *Plant and Vegetation*; Springer: Berlin/Heidelberg, Germany, 2014. [CrossRef]
72. Peel, M.C.; Finlayson, B.; McMahon, T.A. Updated world map of the Köppen-Geiger climate classification. *Hydrol. Earth Syst. Sci.* **2007**, *11*, 1633–1644. [CrossRef]

Disclaimer/Publisher's Note: The statements, opinions and data contained in all publications are solely those of the individual author(s) and contributor(s) and not of MDPI and/or the editor(s). MDPI and/or the editor(s) disclaim responsibility for any injury to people or property resulting from any ideas, methods, instructions or products referred to in the content.